Transition from laminar to turbulent flow in liquid filled microtubes

K.V. Sharp
Department of Mechanical Engineering
The Pennsylvania State University
157D Hammond Building
University Park, PA 16802
814-865-4292
ksharp@mne.psu.edu

R.J. Adrian
Department of Theoretical and Applied Mechanics
University of Illinois at Urbana-Champaign
216 Talbot Lab, MC-262
104 South Wright Street
Urbana, IL 61801
217-333-1793
rjadrian@uiuc.edu

Abstract

The transition to turbulent flow is studied for liquids of different polarities in glass microtubes having diameters between 50 and 247 μm. The onset of transition occurs at Reynolds number ∼1800–2000, as indicated by greater-than-laminar pressure drop and micro-PIV measurements of mean velocity and root-mean-square velocity fluctuations at the centerline. Transition at anomalously low values of Reynolds number was never observed. Additionally, the results of more than 1500 measurements of pressure drop versus flow rate confirm the macroscopic Poiseuille flow result for laminar flow resistance to within -1% systematic and ±2.5% rms random error for Reynolds numbers less than 1800.

1 Introduction

The transition from laminar Poiseuille flow to turbulence in a circular tube is a familiar phenomena that is generally understood to have a minimum lower critical Reynolds number between 1800 and 2300.[1] These values have been established on purely empirical grounds, and traditional linear stability does not adequately predict transition.[2] Nonlinear theories,[3,4] low-dimensional models,[2] and simulations[3,5,6] have been considered to explain and predict transition to turbulence in a circular tube, yet many questions remain open regarding the role of disturbances such as acoustic waves, vibrations, inlet agitation, and molecular motion. Such disturbances do not scale with the diameter of the tube, so one must allow for the possibility of their effect when the diameter is reduced to the sub-100 μm level commonly dealt with in microfluidics.

In microscale flows of liquids the incompressible, viscous Navier-Stokes equations are expected to describe the fluid motion down to scales of the order of 10 molecular spacings,[7] or until the tube diameter drops well below one micron. It is possible that there is a small effect due to slip in the near vicinity of the wall.[8] For hydrophilic boundaries, closer investigations at the wall suggest that the no-slip boundary condition is valid,[9] but even if the wall material is hydrophobic, the slip length is less than 1 μm and the effect of this conservative estimate of slip length on flow resistance is likely to be within any experimental error for flow diameters of the order of 300–400 microns. Other factors, such as such as weak non-Newtonian fluid properties or micro-polar molecular structure, have negligible effects on transition in macroscopic tubes, but might become important in the extremely high shear rates found in microtubes at Reynolds numbers approaching transition. Like the fluctuations described above, these effects also fail to scale only with Reynolds number, and they therefore merit critical examination.

In view of the several factors mentioned above, it is perhaps not surprising that various investigators have interpreted experimentally observed departures from the classical linear relationship between pressure drop and flow rate in microtubes and channels to be a manifestation of anomalous transition to turbulence or non-Newtonian properties. Peng *et al.*[10] based on measured friction factor versus Reynolds number data, report that transition to turbulence occurs as low as Reynolds numbers of 200–700 in rectangular channels with hydraulic diameter 133 to 367 μm, and Mala and Li,[11] again based on measured friction factor versus Reynolds number data, report a departure from expected linear behavior in tubes that may indicate anomalous transition at Reynolds number of 300–900. Other researchers attribute a reduction in expected flowrate to the polar nature of certain liquid molecules for Re$\sim$1–20, $D_h \sim 57$ μm;[12] or they attribute nonlinear pressure drop to surface roughness.[13,14] Wu and Little[14] studied gas flows in channels with $D_h \sim$50–80 μm, Re $\sim$ 200–15000, and Qu *et al.*[13] investigated water flows through trapezoidal channels with $D_h \sim$ 50–170 μm and Re up to 1500. Although Obot[15] reports that there is "hardly any evidence to support the occurrence of transition to turbulence in smooth microchannels for Re $\leq$ 1000", this conclusion is based primarily on his renormalization of Wu and Little's[14] original data. Renormalization is based on an arbitrary dataset which, in this case, is selected to be the conventional friction factor versus Re data. The renormalization is a potentially useful tool in demonstrating a scaling of the friction factor trends, but does not fully address the question of absolute critical Reynolds numbers observed in microchannels. Additionally, although Peng *et al.*[16] suggested early transition based on their data, Obot[15] deduces from the same data that no transitional flow was seen to occur below Re $\leq$ 1000. Despite his deductions based on data from the literature, Obot[15] concludes that "there is a need for carefully crafted experimentation aimed at determining pressure drop.. characteristics."

The purpose of this paper is to report an extensive series of experiments in microtubes with diameters between approximately 50 μm and 250 μm using liquids of different polarities to quantitatively evaluate the effect of scale on the transition from laminar to turbulent flow. To date, the conclusions regarding anomalous transition to turbulence in microchannels have been drawn based on bulk flow measurements in the absence of supporting statistical velocity data. In the current study, it is shown using both bulk flow resistance data and micro-PIV velocity data that over the range of diameters studied, the transition occurs between 1800 and 2300, in agreement with results for large tubes. Thus, at least down to the scale of 50 μm diameter, the transition behaves in a classical manner, unaffected by any of the effects described above.

The experimental study of transition in microchannels is difficult because extreme pressure gradients are needed to achieve the Reynolds numbers at which one expects transition to occur, i.e., ~ 2000. Standard techniques for identifying transition either plot friction factor versus Reynolds number and observe deviations from the laminar relationship or measure RMS axial velocity as a function of Reynolds number and identify the Reynolds number at which the RMS increases above zero. To establish transition by either of these criteria, one must be able to identify, with confidence, the characteristics of laminar microtube flow, a subject that one expects, at first blush, to be trivial. However, the body of experimental knowledge concerning the anticipated laminar flow regime in microtubes is complicated by reports in several investigations of nonlinear relationships between pressure drop and flow rate and/or anomalously high pressure drop, suggestive of turbulent flow. Since transition is, by definition, the departure from laminar flow behavior, it is clear that an investigation of transition cannot proceed without first conclusively establishing the nature of laminar flow in microtubes.

The Darcy friction factor for flow in a duct is defined as

$$f = 2D_h \left(-\frac{dP/dx}{\rho U_B^2} \right) \tag{1}$$

where the hydraulic diameter $D_h = 4A/P$. A is the cross-sectional area, P is the wetted perimeter, ρ is the density, U_B is the bulk velocity, x is the streamwise (axial) direction, and P is the mean pressure. If the fluid obeys Newtonian rheology, the friction factor for steady, fully developed laminar should be given by

$$f = \frac{8C_1}{\mathrm{Re}_{D_h}} \tag{2}$$

where C_1 is a constant that depends on the cross-sectional shape, $\mathrm{Re}_{D_h} = \rho U_B D_h/\mu$ and μ

is the dynamic viscosity.

For a round cross-section, $C_1 = 8$, and the numerator of Eq. 2 has the well-known value of 64. The flow resistance may also be stated in terms of the Poiseuille number, whose definition is

$$\mathrm{Po} \equiv -\frac{1}{\mu}\frac{dp}{dx}\frac{D_h^2}{2U_B} = \frac{f\mathrm{Re}_{\mathrm{D_h}}}{4} = 2C_1. \tag{3}$$

Numerical values of Po for various non-circular channels are tabulated in Sharp *et al.*[17]

Results found in the literature for various cross-sectional shapes are summarized in Fig. 1(a) in which $\mathrm{Po}/2C_1$ is plotted versus Reynolds number. The theoretical laminar value of $\mathrm{Po}/2C_1$ is unity for each cross-section, and the peak scatter exceeds ±40% about this value. The scatter is clearly unphysical and much larger than expected for such simple flows. Part of the scatter in Fig. 1(a) may be associated with using the hydraulic diameter to correlate flow resistance in non-circular cross-sections. However, a plot of Po/16 versus Reynolds number using only the data for circular cross-sections (Fig. 1(b)) reveals similarly large scatter. Hence, the validity of the conventional macroscopic description of flow in these microchannels has been called into question. Having performed their recent resistance experiments in microchannels, Pfund *et al.*[18] stated that "After considering experimental uncertainties and systematic errors, significant differences remained between the results and classical theory." Even more recently, Sobhan and Garimella[19] stated that "Given the diversity in the results in the literature, a reliable prediction of the heat transfer rates and pressure drops in microchannels is not currently possible..".

2 Experiments

2.1 Apparatus

The experimental apparatus, shown in Fig. 2, operated in a manner similar to a blow-down wind tunnel. Liquid from the charged pressure vessel was forced through a long, nearly-constant diameter capillary and collected in a weighing vessel, mounted atop an electronic scale. Measurements of the pressure in the pressure vessel and mass flow rate at the outlet were simultaneously acquired by a computer. The gas pressure in the vessel was recorded using a Validyne CD 15-30 pressure transducer. A Sartorius Model BL310 balance was used to collect the fluid as it flowed out of the capillary tube.

The capillaries used in these experiments were fused silica, externally coated with polyimide, obtained from Polymicro Technologies, with nominal inner diameter ranging from 50 μm to 250 μm. Accurate determination of each capillary diameter was essential to obtain reliable data. The manufacturer's specification of diameter is accurate to within $\pm 6\%$. Optical measurements of the inner diameter of the capillary using end-on views through a 40X objective were only accurate to ± 2.5 μm. SEM measurements, accurate to within $\pm$ 3%, of capillary cross-sectional diameters at various positions along the tubes, indicated variations between 0.7% and 4% over less than 20 mm axial separation. To achieve accurate determination of a length-averaged diameter, direct observations were replaced by experiments, accurate to within $\pm$ 2.5%, that inferred the diameter from the linear (Poiseuille flow) pressure drop versus the flowrate curve in low-Reynolds number region, $20 < \mathrm{Re}_D < 400$ in which the flow clearly obeyed classical behavior with $\Delta p/Q$ constant. (The regions for which $\mathrm{Re}_\mathrm{D} \leq 400$ are noted in Figs. 3(a) and 3(b)). This procedure was verified by comparing measurements of the diameter using different liquids in the same tube. At least two different liquids were used in each of four tubes, and the comparisons of diameter were accurate to within better than 1%. Since data in this range of Reynolds number were used to infer the mean diameter of each tube, we exclude them from the set of data used to characterize the laminar flow that occurs prior to transition, i.e. data for $\mathrm{Re}_D > 400$.

De-ionized water, 1-propanol and a 20% solution by weight of glycerol were used as working fluids, and the total viscosity range was 1.8:1. These liquids have different levels of polarity. Measurements were acquired using $D = 50$–247 μm, and for Reynolds numbers in the ranges 20–400 and 400–2900.

While the measurement of flow resistance in a capillary is simple conceptually, a number of effects can contribute to experimental error, including entrance effects, induced velocity due to streaming potential, microtube compliance, accuracy of the pressure transducer measurement, accuracy of balance measurement, and temperature variations of viscosity. The magnitudes of the individual effects are discussed in Sharp.[20] Taking all errors into consideration, the measurements of Po and f were expected to be accurate to within $\pm 2.5\%$ rms.

2.2 Transition and flow resistance

Before discussing the transition to turbulence, we first show that the laminar flow prior to transition obeyed the the relationships accepted for classical Poiseuille flow in round tubes. The pressure drop versus flowrate data from more than 1500 measurements are summarized in Figs. 1(b), 3(a), and 3(b). In Fig. 3(a), the pressure drop is presented in a dimensionless form,

$$\Delta p^* = \frac{\Delta p}{\frac{32\mu^2 L}{\rho D^3}} \tag{4}$$

versus Reynolds number. Thus, the accepted macroscopic Poiseuille flow result corresponds to $\Delta p^* = \mathrm{Re_D}$. Clearly, the flow resistance depends linearly on the flowrate up to a critical Reynolds number $\mathrm{Re}_{D_{\mathrm{crit}}}$ of approximately 2000. (A magnified view of the data for $\mathrm{Re} \geq 1500$ is presented in Fig. 3(a) in order that the deviations from laminar theory can be better observed.) Below $\mathrm{Re}_{D_{\mathrm{crit}}}$, the data verify the linear dependence of pressure drop on flow rate and viscosity over the full range of Reynolds numbers, and the dependence on diameter is verified for Re_D above 400. (The dependence on diameter is also believed to be correct for Re_D below 400, but since these data were used to determine diameter as discussed previously, the diameter dependence is not strictly verified in the $\mathrm{Re}_D < 400$ region as it is for $400 < \mathrm{Re}_D < \mathrm{Re}_{D_{\mathrm{crit}}}$.)

Fig. 3(b) gives the same results in the conventional form of Darcy friction factor, f, versus Reynolds number, $\mathrm{Re_D}$. This figure is slightly more revealing, in that one can see the measurements falling systematically below the Poiseuille curve for $\mathrm{Re_D}$ above 400. Generally, the measured friction factor agrees to within -1% systematic and ±2.5% rms random error for all experimental Re_D up to transition ($50 < \mathrm{Re}_D < 2000$) for water, 1-propanol, and 20% glycerol flowing through fused silica microtubes with $D \sim 50$ μm–250 μm. Occasional discrepancies larger than the error bars tended to occur in the Reynolds number range $1200 < \mathrm{Re} < 2000$, but in no case is the discrepancy greater than -4%. A likely source of the systematic error lies in the measurement of, or variations in, the diameter of the capillary, but a small microscale physical effect can not be definitively ruled out to within the accuracy of the data. Evenso, for present purposes the data are adequate to prove conclusively that the pressure drop gives absolutely no evidence for transition to turbulence anywhere below the nominal critical value of 2,000.

The present measurements are compared to other experiments in Fig. 1(b). To eliminate any inconsistencies due to channel geometry, the only results presented in Fig. 1(b) are for liquids flowing in circular microtubes. Below $\mathrm{Re}_\mathrm{D} \sim 2,000$ the agreement of the present measurements with the value of unity for laminar Poiseuille is remarkably close when compared with other published results. They scatter about the accepted value almost as much below the critical Re_D as they do above, suggesting that departures from the laminar Poiseuille value in these experiments should not be attributed to transition. In this plot the present data can be seen to begin to systematically increase above $Po/16 = 1$ at $\mathrm{Re}_D = 1800$, but depending on one's definition, the critical Reynolds number could be assigned an value anywhere from 1,800–2,300.

2.3 Transition and the axial velocity

Using the same flow delivery and test sections described previously, micro-PIV experiments were also performed to quantitatively measure the axial, u, component of velocity within the microtubes. In these experiments, a steady pressure was maintained inside the pressure vessel to within ±0.4% to produce very nearly steady flow and thereby to permit time averaging. In all cases, the measurements were obtained at a streamwise location, (x/D)

that was greater than $0.06\mathrm{Re}_D$, the entrance length needed to achieve fully developed flow.[21] Thus, the flow was not expected to change in the streamwise direction across the length of the PIV image, unless there were spatial-time variations due to turbulence or spatial variations due to surface roughness effects. The micro-PIV measurements were capable of detecting fluctuations in t or x, thereby allowing us to assess each effect.

An optical access window, approximately 8 mm in length for each test section, was created by burning off a small section of polyimide coating. To minimize optical distortion resulting from viewing through a curved surface, the optically-accessible measurement volume was encased in a small glass jig with rectangular cross section and filled with water.

Two 15 mJ/pulse Nd:Yag lasers (New Wave, Inc.) provided illumination. The fluorescent particles (diameter ~ 2 μm) had excitation frequencies close to 532 nm, the Nd:Yag wavelength, and emission frequencies in the red spectrum. A filter cube was used to direct the green light entering the back of the microscope through the objective and into the test section, and to prevent stray reflected green (532 nm) light from entering the camera.

A 12-bit cooled TSI PIVCAM 13-8 was used to capture images. This camera has 1280 pixels in the horizontal direction, and 1024 pixels in the vertical direction spaced 6.7 μm in each directions. The time between pulses, Δt, was 3 μs. TSI's Insight 3.2 software controlled the timing and acquisition of all images, PIV SLEUTH software[22] was used to interrogate them. Interrogation windows of 32 pixels by 128 pixels, each containing approximately 5–10 particles, were used in all but the 100.5 μm diameter microtubes. A streamwise offset of up to 80 pixels was used in locating the second interrogation window, depending on the magnitude of U_B. The spacing between vectors was approximately 16 μm in the spanwise direction, except for the smallest diameter case ($D = 100.5$ μm), in which a smaller interrogation windows reduced the spanwise resolution to 8 μm.

The micro- PIV measurements were made in an x–y plane passing through the centerline of the circular microtube (x = streamwise coordinate, $y = 0$ corresponds to the center of the tube in the micro-PIV plane). Despite the steps taken to reduce optical aberration by the walls of the tube, image distortion was significant, so attention was restricted to PIV measurements of $u_{cl} = u(x, 0)$, the velocity on the centerline of the tube where the distortion was a minimum.

Statistics of the centerline velocity were averaged in three ways. The spatial average of a PIV field in the x-direction is denoted by $\langle\ \rangle_x$. The time average over multiple PIV fields taken at separated times is denoted by $\overline{u}$. Combined averages over x and time are denoted by $\langle\overline{u}\rangle_x$. Velocity fluctuations about the time average are denoted by u'.

In Fig. 4 the space-time averaged centerline velocity, $\langle\overline{u}\rangle_x$ normalized by bulk velocity, U_B, is compared, as a function of Reynolds number, to the measurements from two macroscale studies[23,24] of transition in pipe flow. According to Poiseuille theory for fully-developed flow, the measured centerline velocity should be $2U_B$ for Reynolds numbers less than critical, and in this range the present data scatter +/- 10% about the theoretical value. Above the critical Reynolds number in macroscale studies, the centerline velocity decreases smoothly to a value around $1.2U_B$ as the mean velocity profile becomes flatter than parabolic. To within $\pm 10\%$ scatter the micro-scale data generally agree with the macroscopic experiments[23,24] through the transition region. The departure from the laminar value of 2.0 at Reynolds numbers less than critical is not unexpected. As noted by Wygnanski and Champagne,[25] "Deviations from a parabolic profile took place long before any turbulence could be observed."

Unsteady fluctuations of the velocity are clear indicators of the transition to turbulence. The root mean square value of the fluctuating centerline velocity, averaged over x, is plotted in Fig. 5 for test sections with $D \geq 177\ \mu$m. In the definitively laminar region, $\overline{u'^2}$ is expected to be zero. The roughly 1% RMS level observed there is interpreted to be the consequence of slight variations in the total flow rate between PIV frames (0.4%) and measurement noise, which is commonly of order of 1% for PIV measurements. The first evidence of transition, in the form of an abrupt increase in the RMS, occurs between $1800 < \mathrm{Re}_D < 2200$, in full agreement with the flow resistance data. There is no evidence of transition below these values.

The magnitude of the spatial variations in the current experiments, possibly due to wall roughness, is described by the measured rms spatial variation of the centerline velocity, averaged over x, ($\sqrt{\langle(\overline{u}(x,y) - \langle\overline{u}\rangle_x(y))^2\rangle_x}$). The measured rms spatial variation of the centerline velocity, averaged over x and divided by the measured centerline velocity ($\langle\overline{u_{\mathrm{cl}}}\rangle_x$) is plotted versus the Reynolds number in Fig. 6 for all PIV test sections. The root mean square value of the spatial variation is consistent with the 1% noise found in Fig. 5. It is concluded that the magnitude of spatial variations due to roughness are within the noise level, if they exist at all. This implies that although microscale effects are plausible, the differences in microscale and macroscale transition to turbulence in a circular tube are not nearly as large as originally thought by Mala and Li[11] and Peng *et al.*[10] It is concluded that the effects of surface roughness are negligible in the current study.

3 Summary and Conclusions

The flow of a liquid in microchannels should be represented well by continuum theory unless the channel dimensions approach the slip length at the wall, estimated to occur for channels and tubes whose dimensions lay below a few microns. Despite this expectation, significant departures from continuum macroscale theory have been reported in the literature of microfluidics, and they have sometimes been attributed to unknown microscale effects that produce transition to turbulence at anomalously low Reynolds numbers. To resolve this controversy, experiments have been performed in round glass microtubes with diameters ranging from 50 to 247 microns, using liquids with different levels of polarity. The experiments consisted of accurate observation, in more than 1500 cases, of flow resistance measure by pressure drop and flow rate and velocity fluctuations measured by micro-PIV.

The results show conclusively that below a critical Reynolds number for transition to turbulence the flow is described, to within 1% experimental accuracy, by the classical macroscale result for Poiseuille, $f = 64/\mathrm{Re}_D$. More importantly, they show that the transition to turbulence first begins in virtually the same Reynolds number range as that found for macro-scale flow: Re_D =1,800–2,300. Lastly, within the transition range, the behavior of the each microscale flow property — pressure drop, mean velocity and RMS velocity — is consistent with macroscale data. Thus, the behavior of the flow in microtubes, at least down to 50 micron diameter, shows no perceptible differences with macroscale flow. Once demonstrated, the applicability on the microscale of Osborne Reynolds' simple criterion for transition to turbulence may not seem surprising. Evenso, one must be thankful and at least admit to some admiration for a criterion that continues to describe turbulence in, for example, water moving at speeds greater than 150 kph through a tube whose diameter is less than that of a human hair.

Acknowledgements

This work was supported by the Defense Advanced Research Projects Agency, Microsystems Technology Office μFlumes and Composite Computer-Aided-Design Programs, Grant # F33615-98-1-2853.

References

[1] A. G. Darbyshire and T. Mullin, "Transition to turbulence in constant-mass-flux pipe flow," J. Fluid Mech. **289**, 83 (1995).

[2] J. Baggett and L. Trefethen, "Low-dimensional models of subcritical transition to turbulence," Phys. Fluids **9**, 1043 (1997).

[3] P. O'Sullivan and K. Breuer, "Transient growth in circular pipe flow. II. Nonlinear development," Phys. Fluids **6**, 3652 (1994).

[4] L. Trefethen, A. Trefethen, S. Reddy, and T. Driscoll, "Hydrodynamic stability without eigenvalues," Science **261**, 578 (1993).

[5] A. Tumin, "Onset of turbulence in circular pipe flows," in *Laminar-Turbulent Transition*, edited by H. Fasel and W. Saric, IUTAM Symposium (Springer, Sedona, AZ, 1999), pp. 377–382.

[6] A. Lundbladh, D. Henningson, and S. Reddy, "Threshold amplitudes for transition in channel flows," in *Transition, Turbulence and Combustion*, edited by M. Hussaini, T. B. Gatski, and T. Jackson (Kluwer Academic Publishers, The Netherlands, 1994), vol. 1, pp. 309–318.

[7] K. Travis, B. Todd, and D. Evans, "Departure from navier-stokes hydrodynamics in confined liquids," Phys. Rev. E **55**, 4288 (1997).

[8] M. Gad-el-Hak, "The fluid mechanics of microdevices —the Freeman Scholar lecture," J. Fluids Eng. **121**, 5 (1999).

[9] D. Trethway and C. Meinhart, "Apparent fluid slip at hydrophobic microchannel walls," Phys. Fluids **14**, L9 (2002).

[10] X. F. Peng, G. P. Peterson, and B. X. Wang, "Frictional flow characteristics of water flowing through rectangular microchannels," Exp. Heat Transfer **7**, 249 (1994).

[11] G. M. Mala and D. Li, "Flow characteristics of water in microtubes," Int. J. Heat and Fluid Flow **20**, 142 (1999).

[12] I. Papautsky, J. Brazzle, T. Ameel, and A. B. Frazier, "Laminar fluid behavior in microchannels using micropolar fluid theory," Sensors and Actuators **73**, 101 (1999).

[13] W. Qu, G. M. Mala, and D. Li, "Pressure-driven water flows in trapezoidal silicon microchannels," Int. J. Heat and Mass Transfer **43**, 353 (2000).

[14] P. Wu and W. A. Little, "Measurements of friction factor for the flow of gases in very fine channels used for micro miniature joule thomspon refrigerators," Cryogenics **23**, 273 (1983).

[15] N. Obot, "Toward a better understanding of friction and heat/mass transfer in microchannels - a literature review," Microscale Thermophysical Eng. **6**, 155 (2002).

[16] X. Peng, G. Peterson, and B. Wang, "Heat transfer characteristics of water flowing through microchannels," Exp. Heat Transfer **7**, 265 (1994).

[17] K. Sharp, R. Adrian, J. Santiago, and J. I. Molho, "Chapter 6: Liquid flows in microchannels," in *CRC Handbook of MEMS*, edited by M. Gad-el hak (CRC Press, Boca Raton, FL, 2001), pp. 6.1–6.38.

[18] D. Pfund, D. Rector, A. Shekarriz, A. Popescu, and J. Welty, "Pressure drop measurements in a microchannel," J. Fluid Mech. **46**, 1496 (2000).

[19] C. Sobhan and S. V. Garimella, "A comparative analysis of studies on heat transfer and fluid flow in microchannels," Microscale Thermophysical Eng. **5**, 293 (2001).

[20] K. Sharp, "Experimental investigation of liquid and particle-laden flows in microtubes," Ph.D. thesis, University of Illinois at Urbana-Champaign (2001).

[21] F. M. White, *Fluid Mechanics* (Mc-Graw Hill, Inc., New York, 1994).

[22] K. T. Christensen, S. Soloff, and R. J. Adrian, "PIV Sleuth: Integrated Particle Image Velocimetry interrogation/validation software," TAM Report No. 943, Department of Theoretical and Applied Mechanics, University of Illinois at Urbana-Champaign (2000).

[23] V. C. Patel and M. R. Head, "Some observations on skin friction and velocity profiles in fully developed pipe and channel flows," J. Fluid Mech. **38**, 181 (1969).

[24] R. J. Goldstein, R. J. Adrian, and D. K. Kried, "Turbulent and transition pipe flow of dilute aqueous polymer solutions," I. and E. C. Fundamentals **8**, 498 (1969).

[25] I. J. Wygnanski and F. H. Champagne, "On transition in a pipe. Part 1. The origin of puffs and slugs and the flow in a turbulent slug," J. Fluid Mech. **59**, 281 (1973).

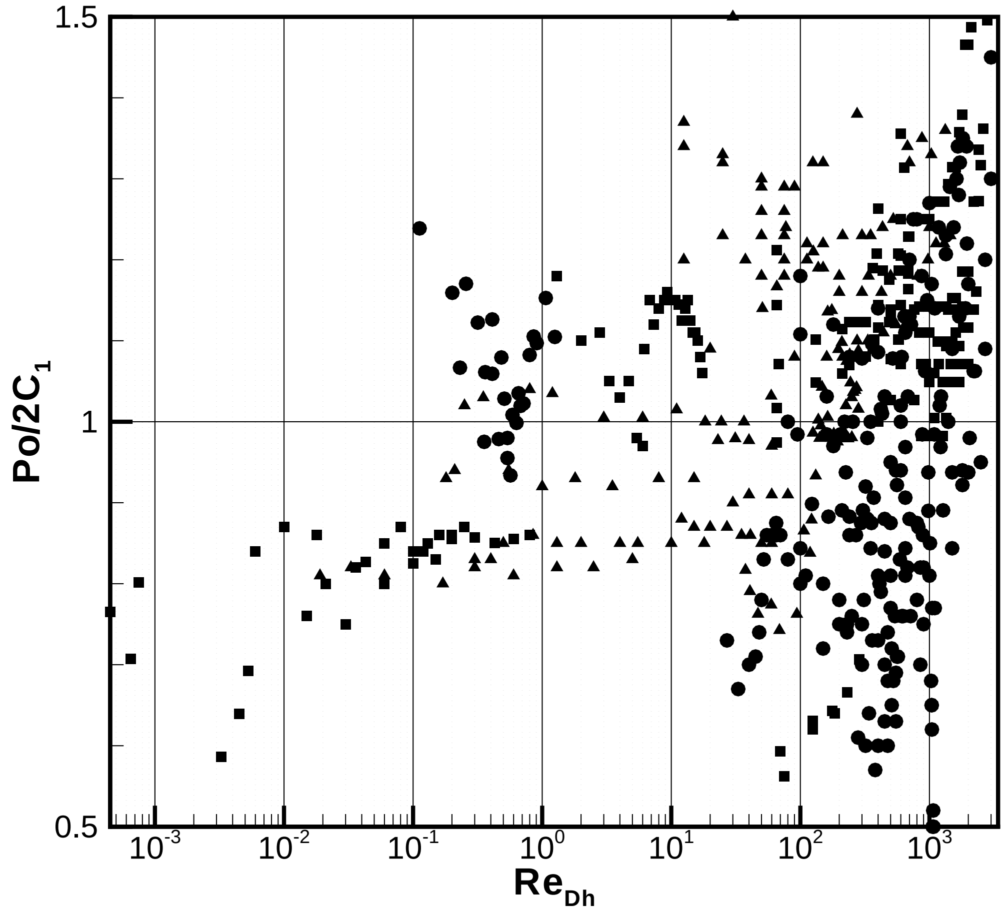

(a)

Figure 1: (a) Comparison of Po/$2C_1$ for microchannels with different channel cross-sections. The theoretical value of Po/$2C_1$ for all geometries is unity. (■) Rectangular channels — [12,18,26,27]; (▲) trapezoidal channels — [13,27–29]; (•) Circular tubes — [11,30–33].

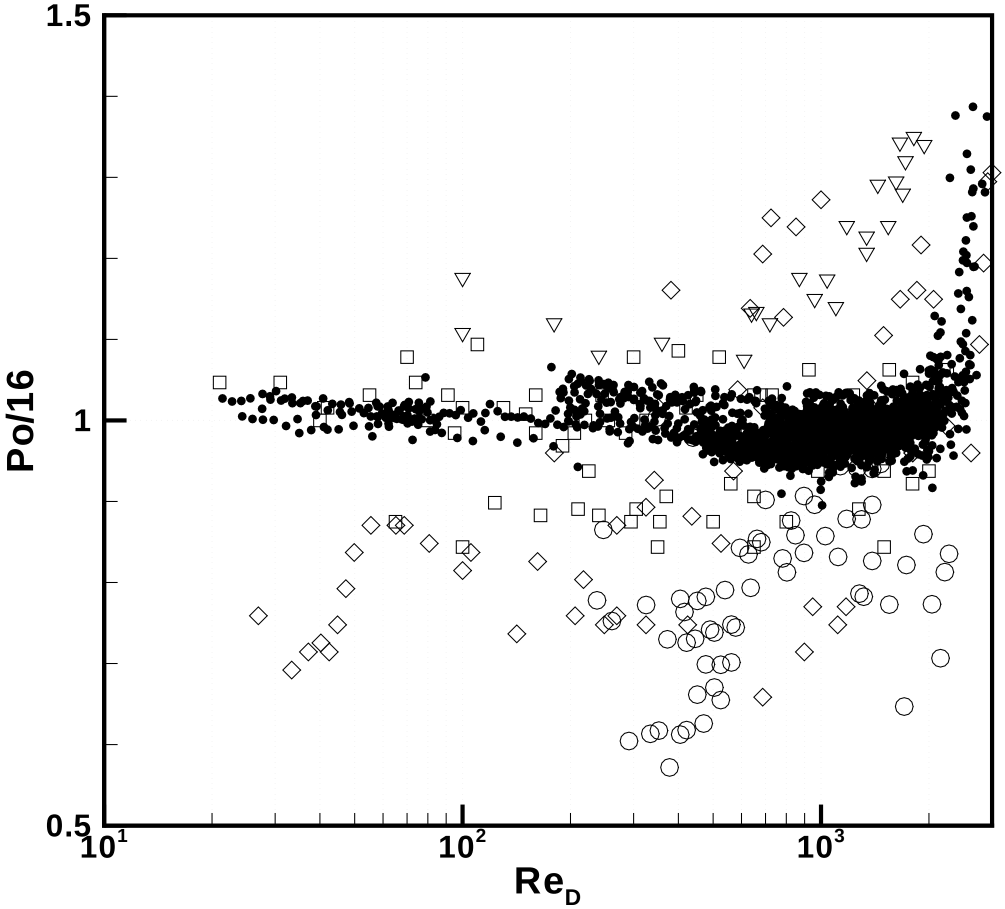

(b)

Figure 1: (b) Po/16 (= Po/$2C_1$), for liquid flows in circular microtubes. (•) current results; (∇) [11]; (○) [32]; (◇) [30]; (□) [33].

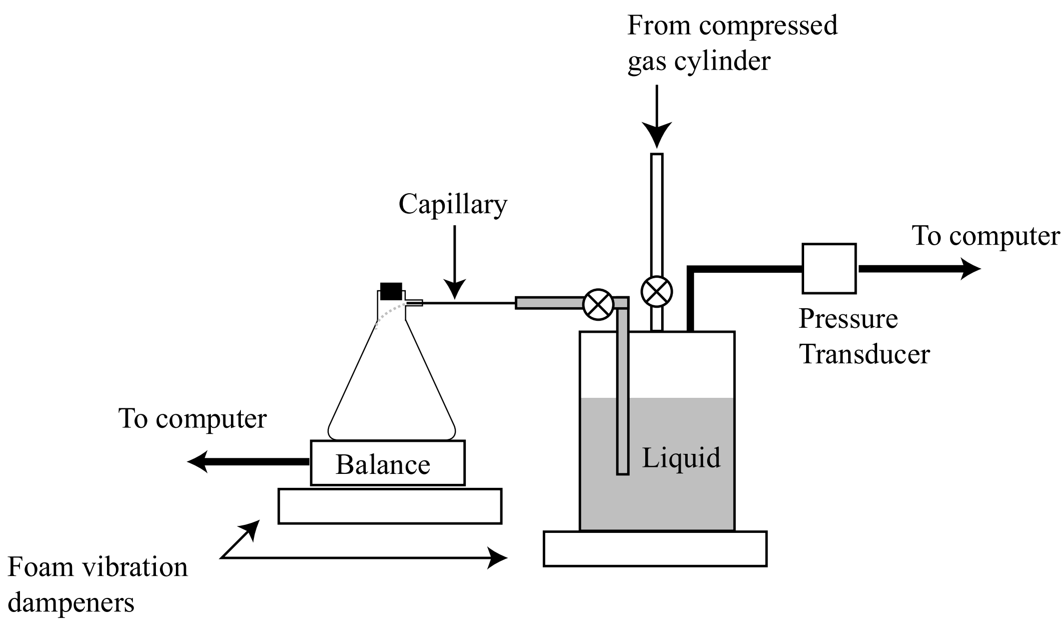

Figure 2: Experimental setup for single-phase flow resistance study using liquid flow driven by gas pressure.

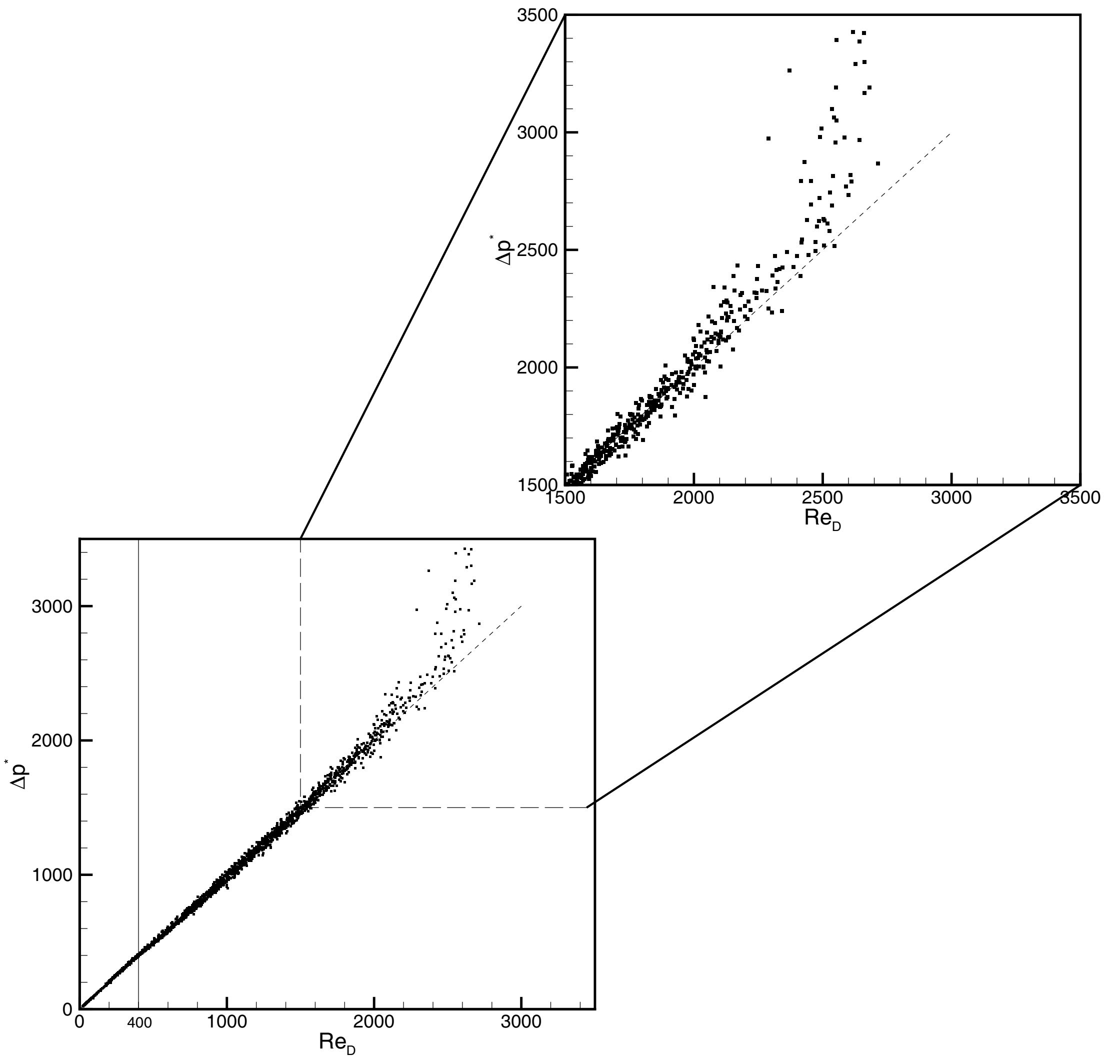

(a)

Figure 3: (a) Normalized pressure drop, Δp^* versus Re_D. The region for which $\mathrm{Re}_D \geq 1500$ is magnified in the inset.

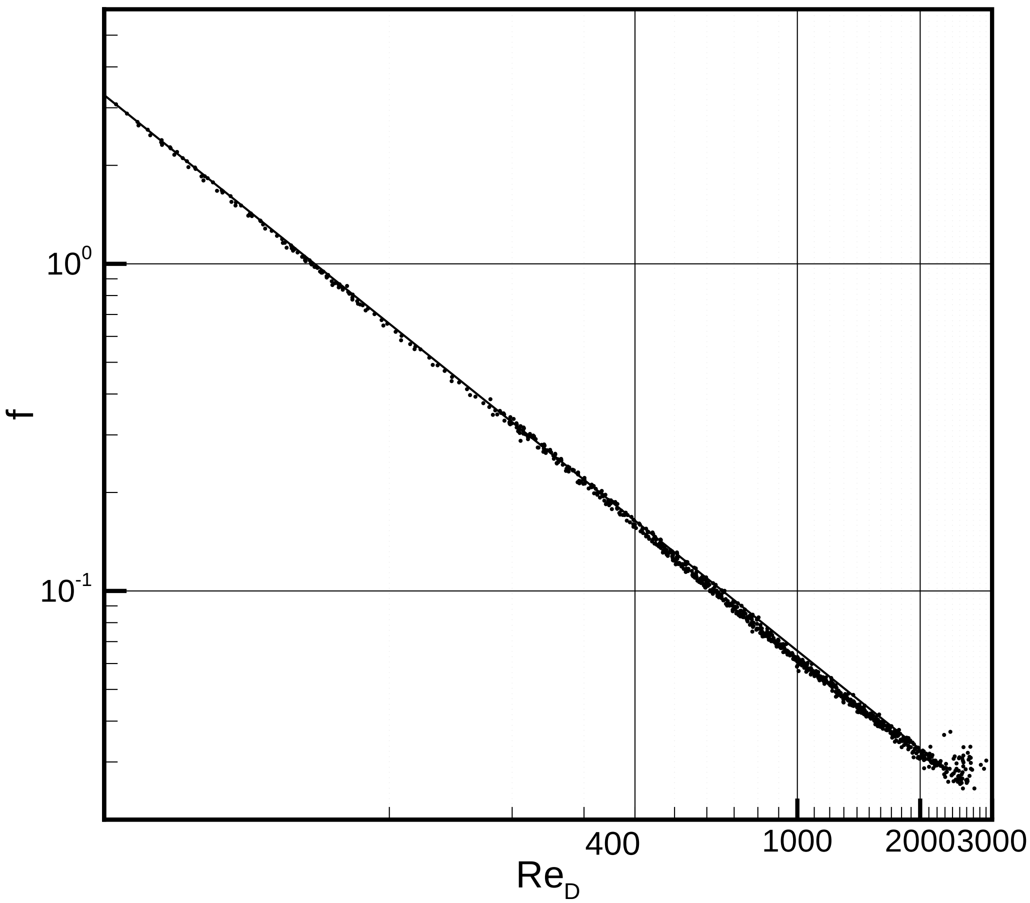

(b)

Figure 3: (b) Friction factor, f, versus Re_D.

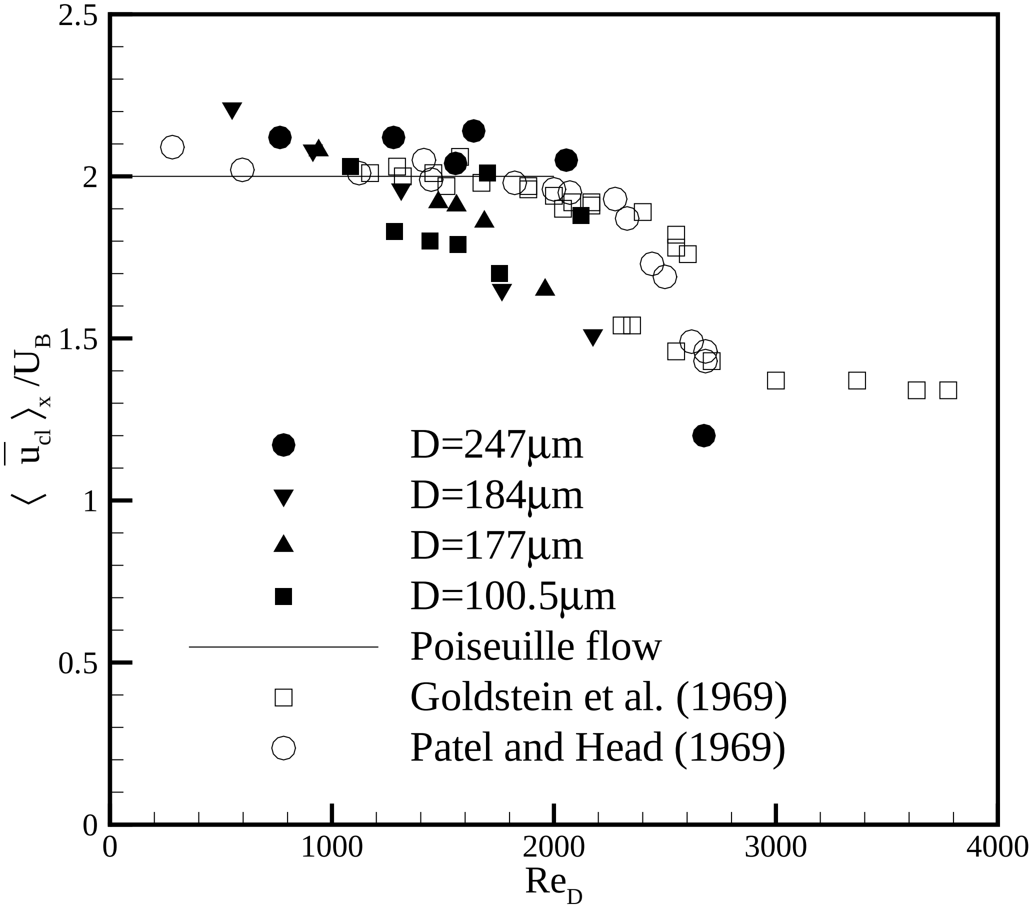

Figure 4: Centerline velocity measured using PIV ($\langle\overline{u_{\text{cl}}}\rangle_x$) divided by the bulk velocity, U_B, versus Re_D.

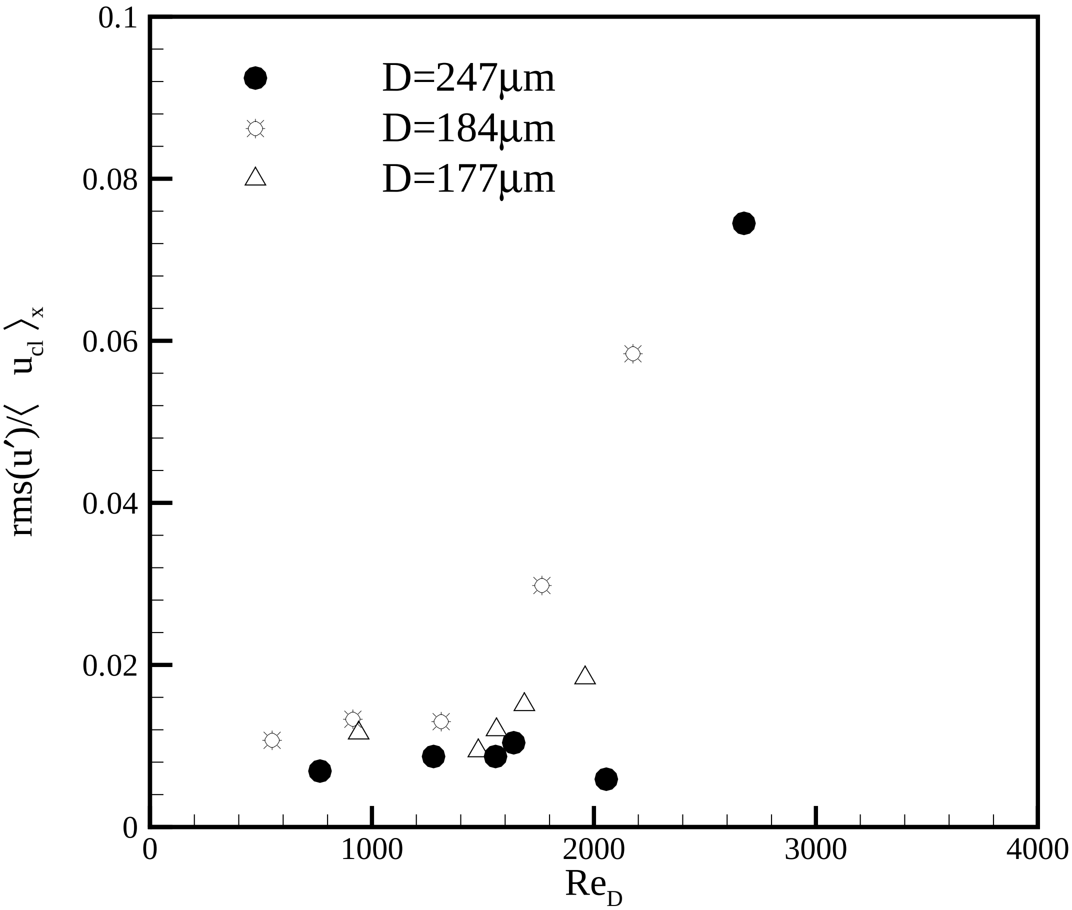

Figure 5: Measured root mean square of the centerline velocity, averaged over x,($\sqrt{\langle\overline{u'^2_{\rm cl}}\rangle_x}$), divided by the measured velocity, ($\langle\overline{u_{\rm cl}}\rangle_x$), versus Re_D.

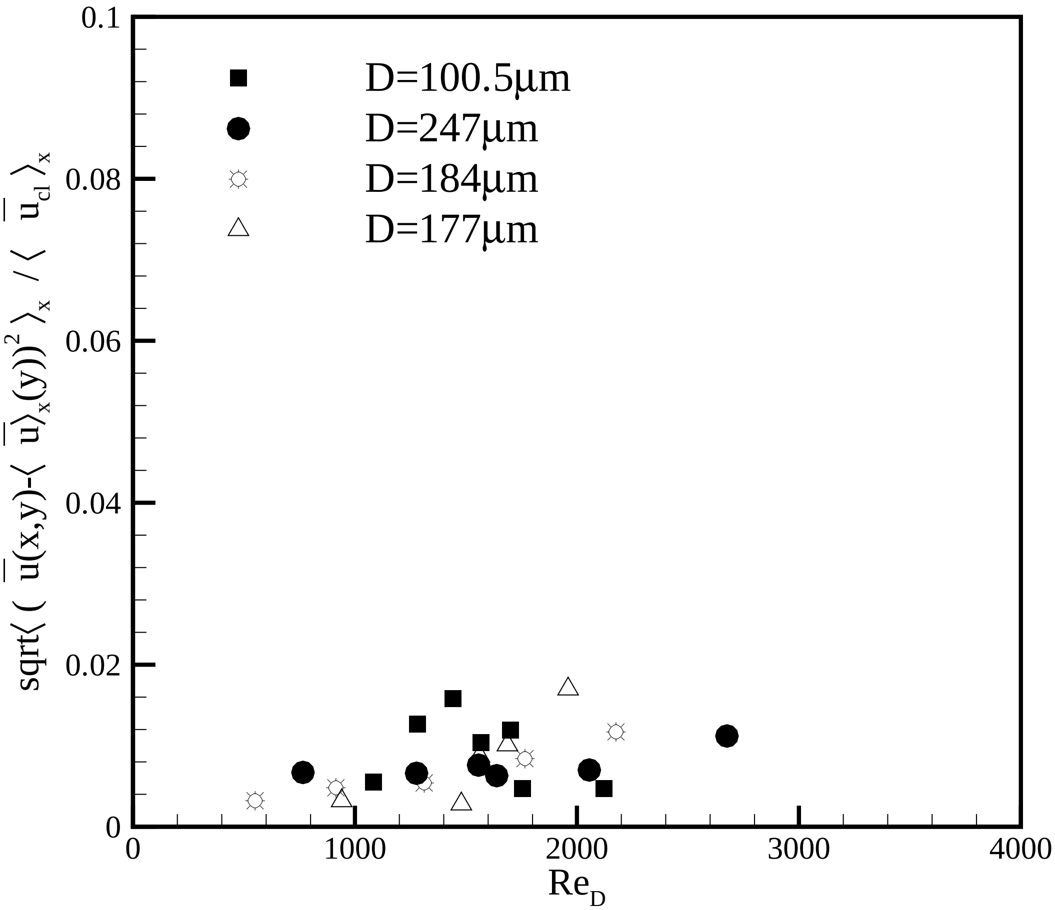

Figure 6: Measured spatial variation of the centerline velocity, averaged over x, $(\sqrt{\langle(\overline{u}(x,y) - \langle\overline{u}\rangle_x(y))^2\rangle_x})$, divided by the measured centerline velocity, $(\langle\overline{u_{\rm cl}}\rangle_x)$, versus Re_D.

List of Recent TAM Reports

No.	*Authors*	*Title*	*Date*
944	Wang, J., N. R. Sottos, and R. L. Weaver	Laser induced thin film spallation—*Experimental Mechanics* (submitted)	May 2000
945	Riahi, D. N.	Magnetohydrodynamic effects in high gravity convection during alloy solidification—In *Centrifugal Materials Processing* (L. L. Regel and W. R. Wilcox, eds.), 317–324 (2001)	June 2000
946	Gioia, G., Y. Wang, and A. M. Cuitiño	The energetics of heterogeneous deformation in open-cell solid foams—*Proceedings of the Royal Society of London A* **457**, 1079–1096 (2001)	June 2000
947	Kessler, M. R., and S. R. White	Self-activated healing of delamination damage in woven composites—*Composites A: Applied Science and Manufacturing* **32**, 683–699 (2001)	June 2000
948	Phillips, W. R. C.	On the pseudomomentum and generalized Stokes drift in a spectrum of rotational waves—*Journal of Fluid Mechanics* **430**, 209–229 (2001)	July 2000
949	Hsui, A. T., and D. N. Riahi	Does the Earth's nonuniform gravitational field affect its mantle convection?—*Physics of the Earth and Planetary Interiors* (submitted)	July 2000
950	Phillips, J. W.	Abstract Book, 20th International Congress of Theoretical and Applied Mechanics (27 August – 2 September, 2000, Chicago)	July 2000
951	Vainchtein, D. L., and H. Aref	Morphological transition in compressible foam—*Physics of Fluids* **13**, 2152–2160 (2001)	July 2000
952	Chaïeb, S., E. Sato-Matsuo, and T. Tanaka	Shrinking-induced instabilities in gels	July 2000
953	Riahi, D. N., and A. T. Hsui	A theoretical investigation of high Rayleigh number convection in a nonuniform gravitational field—*International Journal of Pure and Applied Mathematics*, in press (2003)	Aug. 2000
954	Riahi, D. N.	Effects of centrifugal and Coriolis forces on a hydromagnetic chimney convection in a mushy layer—*Journal of Crystal Growth* **226**, 393–405 (2001)	Aug. 2000
955	Fried, E.	An elementary molecular-statistical basis for the Mooney and Rivlin–Saunders theories of rubber-elasticity—*Journal of the Mechanics and Physics of Solids* **50**, 571–582 (2002)	Sept. 2000
956	Phillips, W. R. C.	On an instability to Langmuir circulations and the role of Prandtl and Richardson numbers—*Journal of Fluid Mechanics* **442**, 335–358 (2001)	Sept. 2000
957	Chaïeb, S., and J. Sutin	Growth of myelin figures made of water soluble surfactant—Proceedings of the 1st Annual International IEEE–EMBS Conference on Microtechnologies in Medicine and Biology (October 2000, Lyon, France), 345–348	Oct. 2000
958	Christensen, K. T., and R. J. Adrian	Statistical evidence of hairpin vortex packets in wall turbulence—*Journal of Fluid Mechanics* **431**, 433–443 (2001)	Oct. 2000
959	Kuznetsov, I. R., and D. S. Stewart	Modeling the thermal expansion boundary layer during the combustion of energetic materials—*Combustion and Flame*, in press (2001)	Oct. 2000
960	Zhang, S., K. J. Hsia, and A. J. Pearlstein	Potential flow model of cavitation-induced interfacial fracture in a confined ductile layer—*Journal of the Mechanics and Physics of Solids*, **50**, 549–569 (2002)	Nov. 2000
961	Sharp, K. V., R. J. Adrian, J. G. Santiago, and J. I. Molho	Liquid flows in microchannels—Chapter 6 of *CRC Handbook of MEMS* (M. Gad-el-Hak, ed.) (2001)	Nov. 2000
962	Harris, J. G.	Rayleigh wave propagation in curved waveguides—*Wave Motion* **36**, 425–441 (2002)	Jan. 2001
963	Dong, F., A. T. Hsui, and D. N. Riahi	A stability analysis and some numerical computations for thermal convection with a variable buoyancy factor—*Journal of Theoretical and Applied Mechanics* **2**, 19–46 (2002)	Jan. 2001

List of Recent TAM Reports (cont'd)

No.	*Authors*	*Title*	*Date*
964	Phillips, W. R. C.	Langmuir circulations beneath growing or decaying surface waves—*Journal of Fluid Mechanics* (submitted)	Jan. 2001
965	Bdzil, J. B., D. S. Stewart, and T. L. Jackson	Program burn algorithms based on detonation shock dynamics—*Journal of Computational Physics* (submitted)	Jan. 2001
966	Bagchi, P., and S. Balachandar	Linearly varying ambient flow past a sphere at finite Reynolds number: Part 2—Equation of motion—*Journal of Fluid Mechanics* (submitted)	Feb. 2001
967	Cermelli, P., and E. Fried	The evolution equation for a disclination in a nematic fluid—*Proceedings of the Royal Society A* **458**, 1–20 (2002)	Apr. 2001
968	Riahi, D. N.	Effects of rotation on convection in a porous layer during alloy solidification—Chapter 12 in *Transport Phenomena in Porous Media* (D. B. Ingham and I. Pop, eds.), 316–340 (2002)	Apr. 2001
969	Damljanovic, V., and R. L. Weaver	Elastic waves in cylindrical waveguides of arbitrary cross section—*Journal of Sound and Vibration* (submitted)	May 2001
970	Gioia, G., and A. M. Cuitiño	Two-phase densification of cohesive granular aggregates—*Physical Review Letters* **88**, 204302 (2002) (in extended form and with added co-authors S. Zheng and T. Uribe)	May 2001
971	Subramanian, S. J., and P. Sofronis	Calculation of a constitutive potential for isostatic powder compaction—*International Journal of Mechanical Sciences* (submitted)	June 2001
972	Sofronis, P., and I. M. Robertson	Atomistic scale experimental observations and micromechanical/continuum models for the effect of hydrogen on the mechanical behavior of metals—*Philosophical Magazine* (submitted)	June 2001
973	Pushkin, D. O., and H. Aref	Self-similarity theory of stationary coagulation—*Physics of Fluids* **14**, 694–703 (2002)	July 2001
974	Lian, L., and N. R. Sottos	Stress effects in ferroelectric thin films—*Journal of the Mechanics and Physics of Solids* (submitted)	Aug. 2001
975	Fried, E., and R. E. Todres	Prediction of disclinations in nematic elastomers—*Proceedings of the National Academy of Sciences* **98**, 14773–14777 (2001)	Aug. 2001
976	Fried, E., and V. A. Korchagin	Striping of nematic elastomers—*International Journal of Solids and Structures* **39**, 3451–3467 (2002)	Aug. 2001
977	Riahi, D. N.	On nonlinear convection in mushy layers: Part I. Oscillatory modes of convection—*Journal of Fluid Mechanics* **467**, 331–359 (2002)	Sept. 2001
978	Sofronis, P., I. M. Robertson, Y. Liang, D. F. Teter, and N. Aravas	Recent advances in the study of hydrogen embrittlement at the University of Illinois—Invited paper, Hydrogen–Corrosion Deformation Interactions (Sept. 16–21, 2001, Jackson Lake Lodge, Wyo.)	Sept. 2001
979	Fried, E., M. E. Gurtin, and K. Hutter	A void-based description of compaction and segregation in flowing granular materials—*Proceedings of the Royal Society of London A* (submitted)	Sept. 2001
980	Adrian, R. J., S. Balachandar, and Z.-C. Liu	Spanwise growth of vortex structure in wall turbulence—*Korean Society of Mechanical Engineers International Journal* **15**, 1741–1749 (2001)	Sept. 2001
981	Adrian, R. J.	Information and the study of turbulence and complex flow—*Japanese Society of Mechanical Engineers Journal B*, in press (2002)	Oct. 2001
982	Adrian, R. J., and Z.-C. Liu	Observation of vortex packets in direct numerical simulation of fully turbulent channel flow—*Journal of Visualization*, in press (2002)	Oct. 2001
983	Fried, E., and R. E. Todres	Disclinated states in nematic elastomers—*Journal of the Mechanics and Physics of Solids* **50**, 2691–2716 (2002)	Oct. 2001
984	Stewart, D. S.	Towards the miniaturization of explosive technology—Proceedings of the 23rd International Conference on Shock Waves (2001)	Oct. 2001
985	Kasimov, A. R., and Stewart, D. S.	Spinning instability of gaseous detonations—*Journal of Fluid Mechanics* (submitted)	Oct. 2001
986	Brown, E. N., N. R. Sottos, and S. R. White	Fracture testing of a self-healing polymer composite—*Experimental Mechanics* (submitted)	Nov. 2001

List of Recent TAM Reports (cont'd)

No.	*Authors*	*Title*	*Date*
987	Phillips, W. R. C.	Langmuir circulations—*Surface Waves* (J. C. R. Hunt and S. Sajjadi, eds.), in press (2002)	Nov. 2001
988	Gioia, G., and F. A. Bombardelli	Scaling and similarity in rough channel flows—*Physical Review Letters* **88**, 014501 (2002)	Nov. 2001
989	Riahi, D. N.	On stationary and oscillatory modes of flow instabilities in a rotating porous layer during alloy solidification—*Journal of Porous Media*, in press (2002)	Nov. 2001
990	Okhuysen, B. S., and D. N. Riahi	Effect of Coriolis force on instabilities of liquid and mushy regions during alloy solidification—*Physics of Fluids* (submitted)	Dec. 2001
991	Christensen, K. T., and R. J. Adrian	Measurement of instantaneous Eulerian acceleration fields by particle-image accelerometry: Method and accuracy—*Experimental Fluids* (submitted)	Dec. 2001
992	Liu, M., and K. J. Hsia	Interfacial cracks between piezoelectric and elastic materials under in-plane electric loading—*Journal of the Mechanics and Physics of Solids* **51**, 921–944 (2003)	Dec. 2001
993	Panat, R. P., S. Zhang, and K. J. Hsia	Bond coat surface rumpling in thermal barrier coatings—*Acta Materialia* **51**, 239–249 (2003)	Jan. 2002
994	Aref, H.	A transformation of the point vortex equations—*Physics of Fluids* **14**, 2395–2401 (2002)	Jan. 2002
995	Saif, M. T. A, S. Zhang, A. Haque, and K. J. Hsia	Effect of native Al_2O_3 on the elastic response of nanoscale aluminum films—*Acta Materialia* **50**, 2779–2786 (2002)	Jan. 2002
996	Fried, E., and M. E. Gurtin	A nonequilibrium theory of epitaxial growth that accounts for surface stress and surface diffusion—*Journal of the Mechanics and Physics of Solids* **51**, 487–517 (2003)	Jan. 2002
997	Aref, H.	The development of chaotic advection—*Physics of Fluids* **14**, 1315–1325 (2002); see also *Virtual Journal of Nanoscale Science and Technology*, 11 March 2002	Jan. 2002
998	Christensen, K. T., and R. J. Adrian	The velocity and acceleration signatures of small-scale vortices in turbulent channel flow—*Journal of Turbulence*, in press (2002)	Jan. 2002
999	Riahi, D. N.	Flow instabilities in a horizontal dendrite layer rotating about an inclined axis—*Proceedings of the Royal Society of London A*, in press (2003)	Feb. 2002
1000	Kessler, M. R., and S. R. White	Cure kinetics of ring-opening metathesis polymerization of dicyclopentadiene—*Journal of Polymer Science A* **40**, 2373–2383 (2002)	Feb. 2002
1001	Dolbow, J. E., E. Fried, and A. Q. Shen	Point defects in nematic gels: The case for hedgehogs—*Proceedings of the National Academy of Sciences* (submitted)	Feb. 2002
1002	Riahi, D. N.	Nonlinear steady convection in rotating mushy layers—*Journal of Fluid Mechanics* **485**, 279–306 (2003)	Mar. 2002
1003	Carlson, D. E., E. Fried, and S. Sellers	The totality of soft-states in a neo-classical nematic elastomer—*Proceedings of the Royal Society A* (submitted)	Mar. 2002
1004	Fried, E., and R. E. Todres	Normal-stress differences and the detection of disclinations in nematic elastomers—*Journal of Polymer Science B: Polymer Physics* **40**, 2098–2106 (2002)	June 2002
1005	Fried, E., and B. C. Roy	Gravity-induced segregation of cohesionless granular mixtures—*Lecture Notes in Mechanics*, in press (2002)	July 2002
1006	Tomkins, C. D., and R. J. Adrian	Spanwise structure and scale growth in turbulent boundary layers—*Journal of Fluid Mechanics* (submitted)	Aug. 2002
1007	Riahi, D. N.	On nonlinear convection in mushy layers: Part 2. Mixed oscillatory and stationary modes of convection—*Journal of Fluid Mechanics* (submitted)	Sept. 2002
1008	Aref, H., P. K. Newton, M. A. Stremler, T. Tokieda, and D. L. Vainchtein	Vortex crystals—*Advances in Applied Mathematics* **39**, in press (2002)	Oct. 2002

List of Recent TAM Reports (cont'd)

No.	*Authors*	*Title*	*Date*
1009	Bagchi, P., and S. Balachandar	Effect of turbulence on the drag and lift of a particle—*Physics of Fluids* (submitted)	Oct. 2002
1010	Zhang, S., R. Panat, and K. J. Hsia	Influence of surface morphology on the adhesive strength of aluminum/epoxy interfaces—*Journal of Adhesion Science and Technology* (submitted)	Oct. 2002
1011	Carlson, D. E., E. Fried, and D. A. Tortorelli	On internal constraints in continuum mechanics—*Journal of Elasticity*, in press (2003)	Oct. 2002
1012	Boyland, P. L., M. A. Stremler, and H. Aref	Topological fluid mechanics of point vortex motions—*Physica D* **175**, 69–95 (2002)	Oct. 2002
1013	Bhattacharjee, P., and D. N. Riahi	Computational studies of the effect of rotation on convection during protein crystallization—*Journal of Crystal Growth* (submitted)	Feb. 2003
1014	Brown, E. N., M. R. Kessler, N. R. Sottos, and S. R. White	*In situ* poly(urea-formaldehyde) microencapsulation of dicyclopentadiene—*Journal of Microencapsulation* (submitted)	Feb. 2003
1015	Brown, E. N., S. R. White, and N. R. Sottos	Microcapsule induced toughening in a self-healing polymer composite—*Journal of Materials Science* (submitted)	Feb. 2003
1016	Kuznetsov, I. R., and D. S. Stewart	Burning rate of energetic materials with thermal expansion—*Combustion and Flame* (submitted)	Mar. 2003
1017	Dolbow, J., E. Fried, and H. Ji	Chemically induced swelling of hydrogels—*Journal of the Mechanics and Physics of Solids*, in press (2003)	Mar. 2003
1018	Costello, G. A.	Mechanics of wire rope—Mordica Lecture, Interwire 2003, Wire Association International, Atlanta, Georgia, May 12, 2003	Mar. 2003
1019	Wang, J., N. R. Sottos, and R. L. Weaver	Thin film adhesion measurement by laser induced stress waves—*Journal of the Mechanics and Physics of Solids* (submitted)	Apr. 2003
1020	Bhattacharjee, P., and D. N. Riahi	Effect of rotation on surface tension driven flow during protein crystallization—*Microgravity Science and Technology* (submitted)	Apr. 2003
1021	Fried, E.	The configurational and standard force balances are not always statements of a single law—*Proceedings of the Royal Society* (submitted)	Apr. 2003
1022	Panat, R. P., and K. J. Hsia	Experimental investigation of the bond coat rumpling instability under isothermal and cyclic thermal histories in thermal barrier systems—*Proceedings of the Royal Society of London A* (submitted)	May 2003
1023	Fried, E., and M. E. Gurtin	A unified treatment of evolving interfaces accounting for small deformations and atomic transport: grain-boundaries, phase transitions, epitaxy—*Advances in Applied Mechanics*, in press (2003)	May 2003
1024	Dong, F., D. N. Riahi, and A. T. Hsui	On similarity waves in compacting media—*Advances in Mathematics Research* (submitted)	May 2003
1025	Liu, M., and K. J. Hsia	Locking of electric field induced non-180° domain switching and phase transition in ferroelectric materials upon cyclic electric fatigue—*Applied Physics Letters* (submitted)	May 2003
1026	Liu, M., K. J. Hsia, and M. Sardela Jr.	In situ X-ray diffraction study of electric field induced domain switching and phase transition in PZT-5H—*Journal of the American Ceramics Society* (submitted)	May 2003
1027	Riahi, D. N.	On flow of binary alloys during crystal growth—*Recent Research Development in Crystal Growth*, in press (2003)	May 2003
1028	Riahi, D. N.	On fluid dynamics during crystallization—*Recent Research Development in Fluid Dynamics* (submitted)	July 2003
1029	Fried, E., V. Korchagin, and R. E. Todres	Biaxial disclinated states in nematic elastomers—*Journal of Chemical Physics* (submitted)	July 2003
1030	Sharp, K. V., and R. J. Adrian	Transition from laminar to turbulent flow in liquid filled microtubes—*Physics of Fluids* (submitted)	July 2003